 CMC, vol.31, no.1, pp.65-85, 2012

Numerical and Experimental Investigation to Reduction of Sedimentation of Particles in MRFs with Permanent Magnets

Chenxi Xiong[1,2], Xianghe Peng[1,2,3], Chunwei Zhao[1,2], Jin Huang[4] and Ning Hu[1,5,6]

Abstract: A method to reduce the sedimentation of the ferromagnetic particles in magnetorheological fluids (MRFs) is studied with numerical simulation and experiment. It shows that, making use of the magnetic field generated by a permanent magnet put simply above an MRF, the sedimentation of the particles in the MRF can be reduced remarkably. The magnetic force on a ferromagnetic particle and that on a particle chain are computed with the finite element (FE) code ANSYS. It reveals that the magnetic force on a particle-chain is much larger than the sum of the magnetic force on each individual particle in the chain without considering the interaction between the magnetized particles. The improvement of the sedimentation stability of MRF samples with permanent magnets is also investigated experimentally with a specially designed testing device, and it is found that a proper choice of the permanent magnet and the distance between the MRF sample and the permanent magnet can efficiently improve the sedimentation stability of MRFs.

Keywords: magnetorheological fluids, sedimentation stability, permanent magnet, numerical simulation, experiment

1 Introduction

Magnetorheological fluids (MRFs) possess superior advantages and have been receiving increasing attention due to their unique magnetorheological (MR) effect. An MRF exhibits good fluidity without applying any external magnetic field, but

[1] Department of Engineering Mechanics, Chongqing University, Chongqing, China
[2] State Key Laboratory of Coal Mine Disaster Dynamics and Control, Chongqing University, Chongqing, China
[3] Corresponding author: Xianghe Peng, *Email address*: xhpeng@cqu.edu.cn
[4] Chongqing Institute of Automobile, Chongqing University of Technology, Chongqing, China
[5] Department of Mechanical Engineering, Chiba University, Chiba, Japan
[6] Corresponding author: Ning Hu, *Email address*: huning@faculty.chiba-u.jp

the property can be changed to that of solid-like materials in a very short time interval once an external magnetic field is applied. When the magnetic field is removed, the fluidity can be recovered immediately [Bossis *et al.* (2002); Peng and Li (2007)]. Because of this particular characteristic, MRFs have been used for the purpose of semi-active control in many fields [Jin *et al.* (2005); Janocha (2001); Carlson (2000)]. However, there is a bottleneck for MRFs to be applied more extensively in practice, i.e., the sedimentation of the suspended ferromagnetic particles due to the big difference between the apparent density of particles and that of carrier fluid. Although a lot of efforts have been made [Viota *et al.* (2007); Alves *et al.* (2009); Park *et al.* (2006); Yang *et al.* (2006)], this problem remains unsolved. At the present stage, a common method to enhance the sedimentation stability of MRFs is addition of appropriate additives [López-López *et al.* (2006, 2007, 2008)]. This method has some obvious disadvantages: since there is no mature theory for how to use different types of additives in different MRFs, a lot of trial experiments are needed to determine the proper type and quantity of additives. Thus, this method is neither time-saving nor economic. On the other hand, no available additive has been found that could permanently solve the sedimentation problem. Some other methods, such as wrapping the particles with light-weighted coatings or using hollow particles to reduce the apparent density of the particles [Pu *et al.* (2006); Choi *et al.* (2006); Jiang *et al.* (2006); Choi *et al.* (2007); Luo and Liu (2007)], and adding nano-size particles [Park *et al.* (2006); Fang *et al.* (2007)], etc., have also been studied, but there are still many unsolved problems related to their applications.

In this work, a method to enhance the sedimentation stability of MRFs is studied. It is based on the proverbial fact that a ferromagnetic particle near a permanent magnet would be attracted by it. When a permanent magnet is put above an MRF, it can provide a ferromagnetic particle with an upward magnetic force. If the force could suitably counteract gravity, the particle would stop settling. This method is investigated in two ways: (1) the magnetic force between a ferromagnetic particle or a particle-chain and a permanent magnet is analyzed, and the suitable magnetic field for the sedimentation stability of MRFs is analyzed; and (2) the validity of this method is verified with experiment. Some problems related to the application of the proposed method in practical MRF devices are also discussed.

2 Numerical Simulation

2.1 Finite element model

In this section, the finite element method (FEM) is used to analyze the magnetic force induced by a permanent magnet on a single ferromagnetic particle or a ferro-

magnetic particle chain. Compared with the result obtained with magnetic dipolar model [Peng and Li (2007)], the result obtained with FEM can provide some more essential information, since FEM can simulate more realistically the distribution of magnetic field in the particle(s), the nonlinear magnetization effect and partial saturation magnetization of a ferromagnetic particle, and the interaction between magnetized particles.

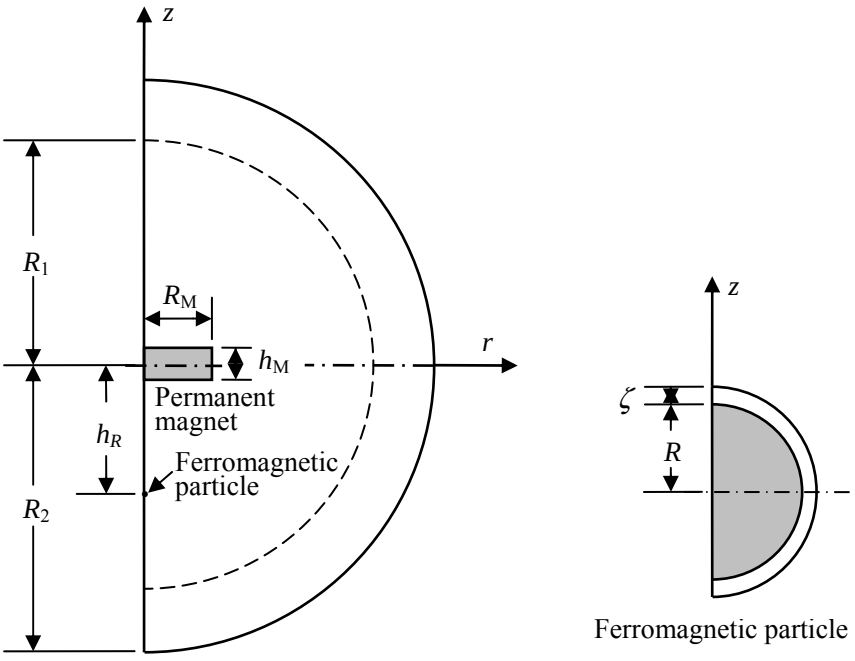

(a) Entire model (b) Particle (R = 5 μm)

Figure 1: Set-up of permanent magnet - particle system for FE analysis

A model includes a permanent magnet, a ferromagnetic particle and the surrounding air. The particle is located away from the permanent magnet at a prescribed distance, h_R, as shown in Fig. 1. The magnetic force on the particle can be obtained by calculating the integral of the Maxwell stress tensor over its surface [Ly *et al.* (1999)], and then the magnetic force on an entire chain formed by ferromagnetic particles located at different distances from the permanent magnet can be obtained.

Picking a ferromagnetic particle, its center is located on the vertical line passing through the center of the permanent magnet. The radius and the height of the permanent magnet are $R_M$and h_M, respectively. The FEM model is considered axisymmetrical, as shown in Fig. 1. The particle of radius R wrapped by a non-magnetic coating of thickness is located at $r=0, z=-h_R$. Considering a smooth transition of element density, the surrounding air is divided into several layers. A far-field layer with thickness R_2-R_1 is set to simulate the far-field dissipation of the magnetic field. The demagnetization curve of the permanent magnet is simplified as a straight line, therefore, its property can be determined with the relative permeability μ_r^M and the coercive force vector $\mathbf{H}_c$. The permanent magnet is magnetized in the direction of its thickness; hence the coercive force vector is in the same direction as the $z-$axis. The $B-H$ curve of pure iron shown in Fig. 2 is used for the particles, and the other parameters used are listed in Table 1.

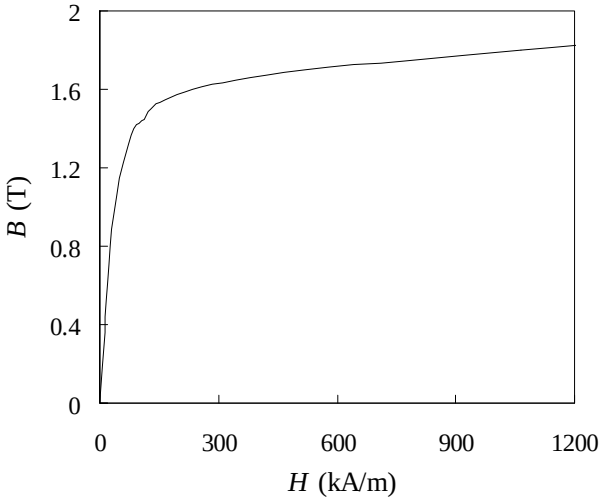

Figure 2: Magnetization curve of ferromagnetic particle

Table 1: Parameters used in simulation.

R_M(mm)	h_M(mm)	$R(\mu$m)	ζ (μm)	R_1(mm)	R_2(mm)	μ_r^M	H_c(kA/m)
20	10	5	1	70	90	1.02	955

2.2 Results and discussion

The distribution of the magnetic field intensity, H, is computed with the finite element (FE) code ANSYS. Figures 3 and 4 show respectively the contour map of H in the entire model and that near the particle, with $h_R = 42$mm. It can be seen in Fig. 3 that the maximum value of H appears near the right top corner of the permanent magnet, and decreases with the increase of the distance from the permanent magnet. The ferromagnetic particle does not distinctly affect the overall magnetic field, but changes the local magnetic field nearby (Fig. 4). It can be seen in Fig. 4 that, in the right side of the dotted line about 40 μm from the particle, the effect of the magnetized particle on H is insignificant. In the air near the two poles of the particle H is enhanced markedly; while in the air near the equator, H decreases to about half the normal value. It can be attributed to the additional magnetic field induced by the magnetized particle, which is in the same direction as the permanent magnet's magnetic field on the $z-$axis, so it can strengthen the entire magnetic field; but near the equator of the particle, the additional magnetic field is in the opposite direction against the applied magnetic field.

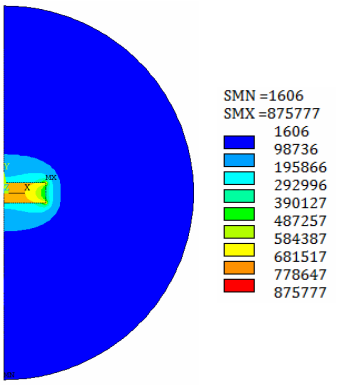

Figure 3: Distribution of H (A/m)

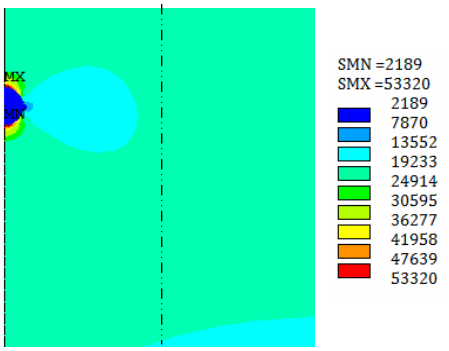

Figure 4: Contour map of H(A/m) near the particle (The width of the figure is 88 μm)

The magnetic force on the magnetized particle at different h_R can be computed. In an axisymmetrical case, only the $z-$component of the magnetic force remains. If λ is defined as the ratio of the magnetic force F^b to the sedimentation force F^d, calculated by subtracting buoyancy from gravity of the particle, then λ can serve as the parameter indicating the sedimentation state of a particle. Since in this simulation the carbonyl iron particles are used for the disperse phase, the apparent density of the particle ρ=7.5g/mm^3, given R=5mm, the density of the carrier liquid

ρ_c=0.98g/mm^3, and the acceleration of gravity$g$= 9.8m/s^2, the sedimentation force of each particle can be calculated with

$$F^d = \frac{4}{3}\pi R^3(\rho - \rho_c)g = 3.346 \times 10^{-11}\text{N}$$

The variation of λ against h_R (40mm$\leq h_R \leq$50mm) is computed and shown in Fig. 5. In this interval, F^b changes from 5.000×10^{-11} at h_R=40mm to 1.394×10^{-11}N at h_R=50mm, i.e., F^b decreases as h_R increases. It can be seen that F^b=3.346$\times 10^{-11}$N at $h_R \approx$43.0mm, i.e., λ = 1 (Fig. 1), indicating that the particle at $h_R \approx$43.0mm may suspend stably. More refined analysis for the λ near $h_R \approx$43.0mm will be performed and the result is shown in Fig. 6, where it can be seen that F^b varies almost linearly against h_R and can be approximated with

$$F^b = -4.35 \times 10^{-12} h_R + 2.205 \times 10^{-10}. \quad (1)$$

The balance between F^b and F^d at h_R=43.0mm also indicates that an individual particle could not be separated from the MRF by the magnetic force, and h_R=43.0mm will, therefore, be used as a reference position to analyze the magnetic force on an entire chain.

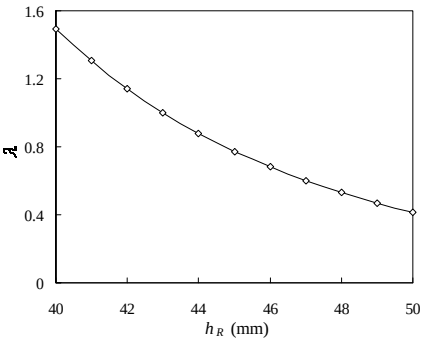

Figure 5: λ-h_R curve

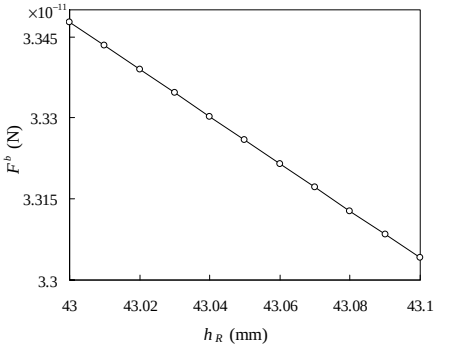

Figure 6: Variation of F^b against h_R near λ=1

In a magnetic field the dispersed ferromagnetic particles suspended in a carrier fluid can be magnetized and aggregate to form chain or column structures. This has already been observed experimentally [Zhu *et al.* (1996); Furst *et al.* (2000); Tang *et al.* (2000); Rong *et al.* (2000)] and simulated numerically [Peng and Li (2007); Ly *et al.* (1999); Keaveny *et al.* (2008); Li *et al.* (2008); Vladimir *et al.* (2006); Ekwebelam and See (2009); Li *et al.* (2005)]. In order to simplify the numerical process,

we assume in the analysis a straight chain of n particles arranged in the direction of the magnetic field [Peng *et al.* (2007); Li *et al.* (2005)]. It should be noted that although the realistic behavior should also be affected by many other influencing factors, such as the dispersivities of the particle shape and size, the orientation of particle chains, the defects in chains and the interaction between chains, and other kinds of possible microstructures, the results based on this assumption can provide, at least, a reasonable approximation and some available information for the case with relatively low particle volume fraction, and a reference for other cases [Li *et al.* (2005); Xiong *et al.* (2011)].

In a magnetic particle chain, the magnetic force on a ferromagnetic particle also strongly depends on the other magnetized particles. Therefore, we analyze the behavior of an entire chain under a permanent magnet with ANSYS. Assuming the particles in a chain are of identical spheres, there are three parameters determining the geometry of such a chain: the distance h_R between the center of the permanent magnet and the topmost particle in the chain, the distance $l$between two adjacent particles, and n, the number of particles in the chain. In the following example, n = 8, h_R=43.0mm, and l=13μm (2R=10μm, 2ζ=3μm) are adopted.

Figure 7 shows the contour map of the magnetic field intensity near the chain, comparing with Fig. 4, it can be seen that both the range and the intensity of the magnetic field increase remarkably. The change in the magnetic filed near the chain appears similar to that in the case of a single particle.

Magnetic field intensity in the eight particles (Fig. 7) is shown in Fig. 8(a), where it can be seen that, because of the interaction of magnetized particles, the magnetic field intensity in each of the particles increases compared with the result of one single particle. The magnetic field intensity in each of the six middle particles in the chain is markedly enhanced at its two poles, but the magnetic field intensity in either of the end particles of the chain is not symmetric. Figure 8(b) shows the magnetic field intensity in the third particle from the top, which is strong at its two poles but weak at its flank. Computation shows that the magnetic field intensity at the lower pole is a little larger than that at the upper pole even if the top pole is closer to the permanent magnet, which can be attributed to that there are 2 particles above it and 5 below it, indicating the significance of the effect of the magnetized particles. If the particles from top to bottom are numbered sequentially with M1 to M8, the magnetic force, F^b, on each single particle is calculated and listed in Table 2.

It can be seen that, the magnetic force on the particles close to the end of the chain is larger than that on the particles close to the center of the chain, and the difference can span several orders of magnitude. F^b can further be separated into two parts: the magnetic force ${F^b}_M$ induced by the gradient magnetic field generated

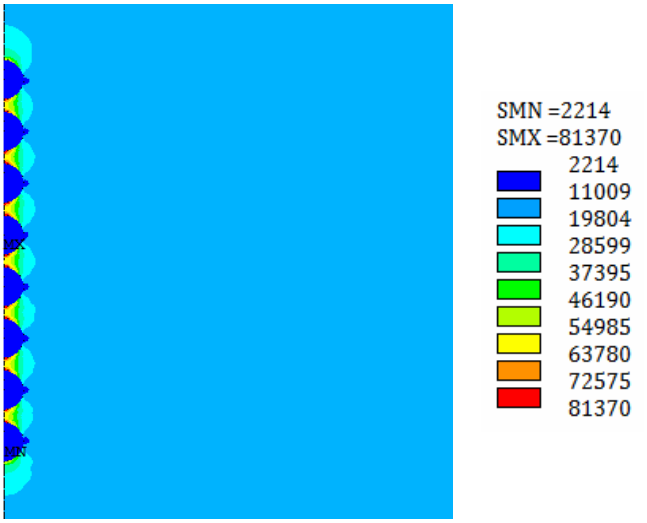

Figure 7: Contour map of magnetic field intensity near a particle chain (A/m) (The actual width of the figure is 0.1mm)

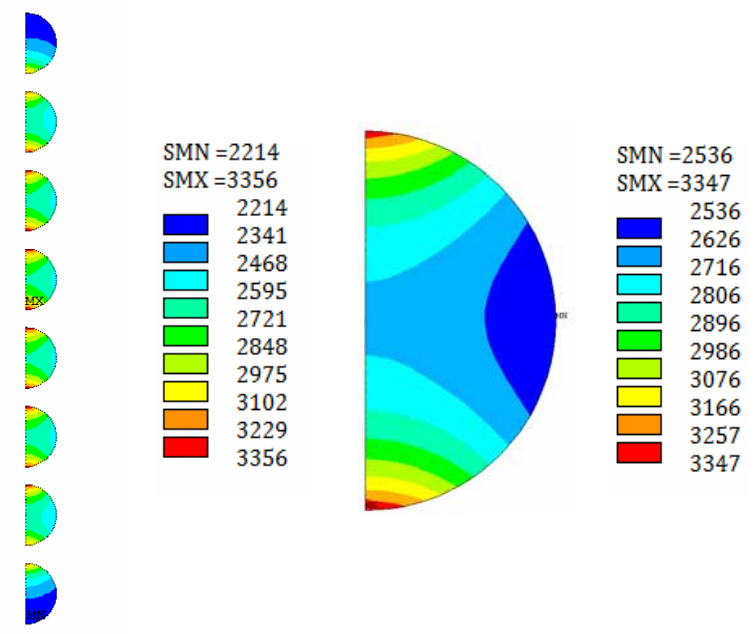

(a) The chain (b) The 3rd particle

Figure 8: Contour map of magnetic field intensity in particles (A/m)

Table 2: Magnetic force on particles

Serial number	F^b(N)	h_R (mm)	F^b_{M}(N)	F^b_i(N)
M1	-2.3719E-08	43	3.3477E-11	-2.37525E-08
M2	-3.8972E-09	43.013	3.34205E-11	-3.93062E-09
M3	-9.1017E-10	43.026	3.33639E-11	-9.43534E-10
M4	-3.2008E-11	43.039	3.33074E-11	-6.53154E-11
M5	3.0232E-10	43.052	3.32508E-11	2.69069E-10
M6	1.2535E-09	43.065	3.31943E-11	1.22031E-09
M7	4.1879E-09	43.078	3.31377E-11	4.15476E-09
M8	2.3569E-08	43.091	3.30812E-11	2.35359E-08
ΣF^b	7.5384E-10			

by the permanent magnet, and the magnetic force ${F^b}_i$ induced by the additional magnetic field by the other magnetized particles. For the particle at the end of the chain, the contribution to ${F^b}_i$ by any other particle has the same direction, which accounts for the comparatively large value of ${F^b}_i$. For the particles inside the chain, the contributions to ${F^b}_i$ by other particle may have opposite direction and may counteract each other to a certain extent, accounting for the smaller value of ${F^b}_i$ on these particles.

The values of h_R for the eight particles are also given in Table 2. Compared with the h_R in Fig. 6, it can be seen that the values of h_R in Table 2 are almost in the range of the h_R in Fig. 6, and the approximation Eq. (1) is available for the estimation of ${F^b}_M$ on each particle, and ${F^b}_i$ can be obtained by subtracting ${F^b}_M$ from F^b.

The sum of the magnetic force on the particles in the chain is shown in the last row of Table 2. The magnetic force on the entire chain is 7.538×10^{-11}N, on the other hand, the sedimentation force of the chain is 2.676×10^{-10}N. This result suggests that, in the magnetic field provide by a permanent magnet, the chain structure formed can enhance effectively the capability against the sedimentation of ferromagnetic particles.

The magnetic forces ΣF^bon the chains with different n are computed and shown in Table 3, where the sedimentation force ΣF^d and the ratio λ are also shown for comparison. In all the chains, the topmost particles are located at h_R=43.00mm, where the magnetic force on an individual single particle equals its sedimentation force. Since the other particles are below this position, the magnetic force on each individual single particle should be less than its sedimentation force. However, as these particles form a chain, the magnetic force on the chain, ΣF^b, is not less than sedimentation force. In Table 3, ΣF^b is greater than ΣF^d in each case. λ>1

Table 3: Magnetic forces of chains containing different number of particles

n	$\sum F^b$(N)	$\sum F^d$(N)	λ
1	3.3477E-11	3.34559E-11	1.00063
4	1.7584E-10	1.33824E-10	1.31397
6	4.2301E-10	2.00735E-10	2.10730
8	7.5384E-10	2.67647E-10	2.81654
15	1.4277E-09	5.01839E-10	2.84494
20	2.2274E-09	6.69118E-10	3.32886
50	1.4117E-08	1.6728E-09	8.43917
75	2.32E-08	2.50919E-09	9.24600
90	2.5371E-08	3.01103E-09	8.42602
110	3.035E-08	3.68015E-09	8.24695
150	2.6609E-08	5.01839E-09	5.30230

even if n=150. This result is definitely beneficial for the sedimentation stability of MRFs. In practical application, the range for the sedimentation stability might be further extended, provided the permanent magnets are properly chosen and set and the chain structures can form satisfactorily.

The variation of λ of the chain containing 90 particles against h_R is shown in Fig. 9. The magnetic force on the chain decreases with the increase of h_R. λ tends to unit when h_R increases to 63.00mm. Comparing to the reference position h_R= 43.00mm, this position is extended by about 20mm.

3 Experiment

3.1 Method and device

In order to verify the validity of the proposed method, a testing device is prepared, as shown in Fig. 10, where a tube of a uniformly stirred MRF is placed vertically beneath the center of a permanent magnet. Another tube of the same sample without using any permanent magnet is also prepared for comparison.

Two parameters that may affect the experimental results are: the distance from the bottom of the permanent magnet to the surface of the MRF sample, h_1, and the height of the MRF sample in the tube, h_2. The value of h_1 takes the data determined with the FE simulation.

The tube containing the MRF sample is marked with scales, with the inner diameter 10 mm and the length 55 mm. The MRF sample used is composed of carbonyl iron powder and silica oil, without any additive. The volume fraction of iron powder is

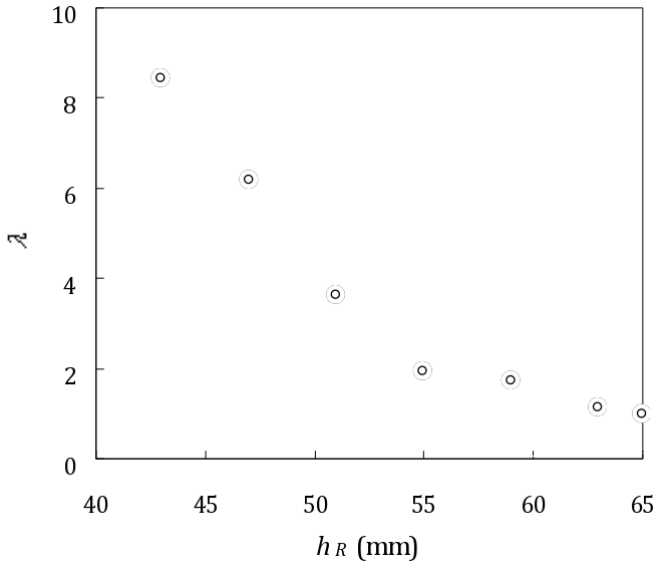

Figure 9: λ-h_R curve of a chain when n=90

less than 10%, so the sedimentation stability of the sample should be very poor. It can completely settle within two days.

The vertical competent of the magnetic flux density induced by the permanent magnet, B_z, is measured with a Gauss meter. All measuring points are on the vertical line passing through the center of the permanent magnet. The measuring results are shown in Fig. 11, in which the abscissa is the distance between the point and the bottom of permanent magnet, h.

The sedimentation stability of the MRF sample can be evaluated with the sedimentation ratio defined as $S = \frac{h_3}{h_2} \times 100\%$, where h_3 (Fig. 12) is the height of the upper layer where the ferromagnetic particles have almost settled. Such a layer may always appear in an MRF sample after a certain time interval due to sedimentation.

3.2 Results and discussion

For the test without a permanent magnet, corresponding to h_1=∞, setting h_2=28mm, the sedimentation of the sample is observed and used as reference. The observed sedimentation is shown in Fig. 13, where it can be seen that the sedimentation ratio $S \approx 50\%$ in the first half day; and $S \approx$68.3% in the first day; after the first day, no further sedimentation can be observed. Therefore, the average daily sedimentation ratio of the MRF sample without using a permanent magnet is about 68.3%.

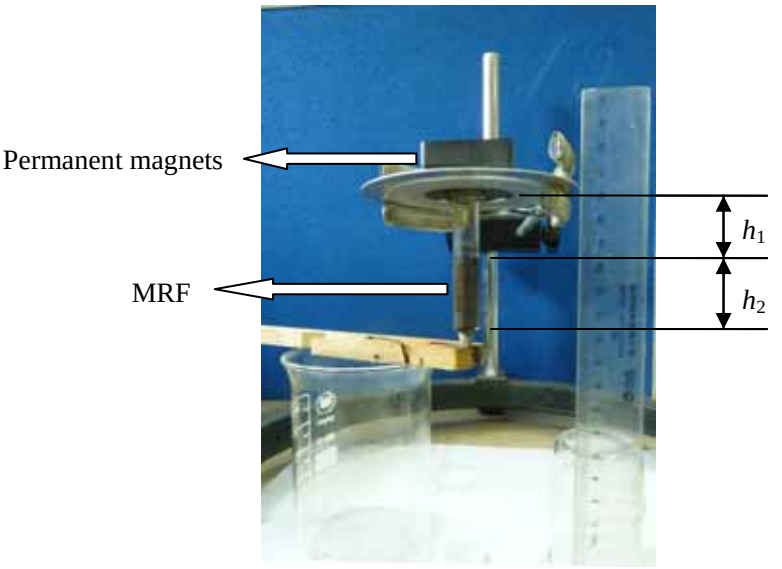

Figure 10: Setup of experiment

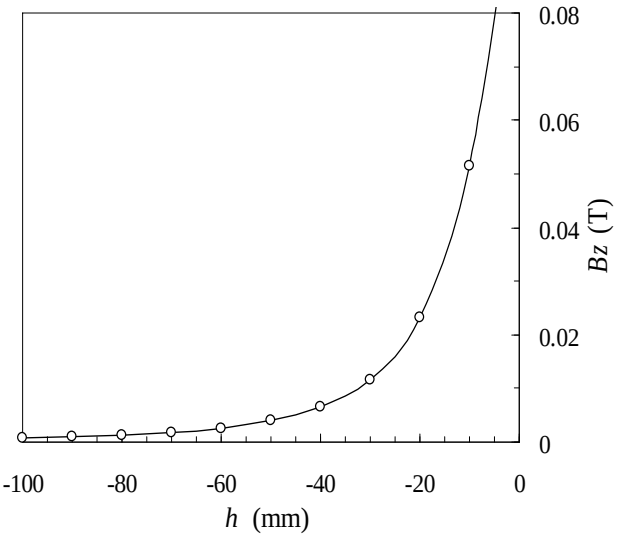

Figure 11: B_z- h curve

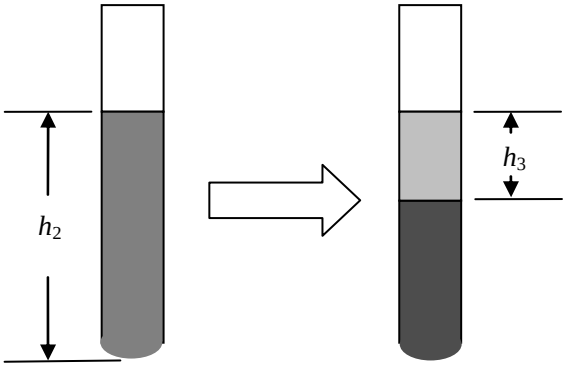

Figure 12: Sedimentation of MRF sample

If a permanent magnet is simply put above the MRF with h_1=35mm and h_2=24mm, the sedimentation of the sample is shown in Fig. 14. It shows that $S\approx$ 20.5% in the first day, and the rate of S decreases day by day. The sedimentation stops in about three days, and the average daily sedimentation ratio is reduced to about 13.0%.

If h_1 is further decreased to 29mm, setting h_2=29mm, the sedimentation of the sample is observed and shown in Fig. 15. It can be seen that the sedimentation rate further decreases and the average daily sedimentation ratio is reduced to about 8.1%.

Figure 16 shows the sedimentation of the MRF sample with h_1=26mm and h_2=33mm. The sedimentation velocity tend to be very small, no distinct stratification can be observed by naked eye within 48 hours, and average daily sedimentation ratio falls to about 2.3%.

If h_1 is further decreased to 24 mm, and setting h_2=35mm, the sedimentation of the sample is shown in Fig. 17. The sedimentation can hardly be observed with naked eye even in 8 days, indicating that the sedimentation ratio is zero. If we then remove the permanent magnet and make the sample be under the same condition as that of the reference one. The sedimentation of the sample in the following three days is shown in Fig. 18. It can be seen that the sedimentation is quite similar to that of the reference case. The sedimentation ratio in the first day is about 66.4%, which indicates that the internal structure of MRF is not markedly changed after 8-day test with a permanent magnet.

If h_1 is further reduced to 22 mm, it can be seen that some ferromagnetic particles would separate from the sample and adhere to the bottom of the permanent magnet. It can be attributed to that the magnetic force on the particle is so large that the sedimentation force and the additional magnetic force induced by the other magnetized

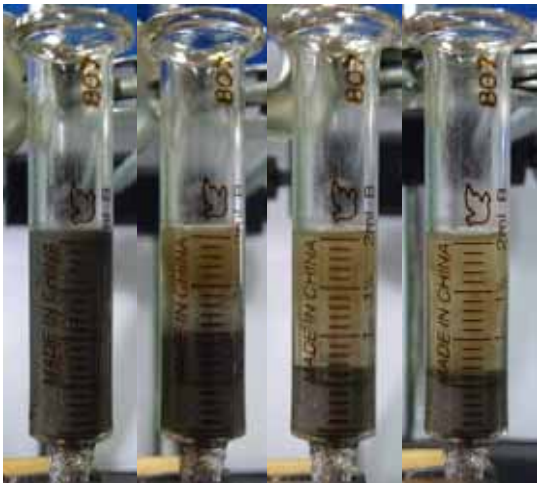

0d 0.5d 1d 2d

Figure 13: Sedimentation of MRF (h_1=∞, h_2=28mm) sample, without a permanent magnet

0d 0.75d 1.25d 2d 3d 3.75d

Figure 14: Sedimentation of MRF, with h_1=35mm and h_2=24mm

0d 1d 1.5d 2d

Figure 15: Sedimentation of MRF, with h_1=29mm and h_2=29mm

0d 1d 2d 3d

Figure 16: Sedimentation of an MRF, with h_1=26mm and h_2=33mm

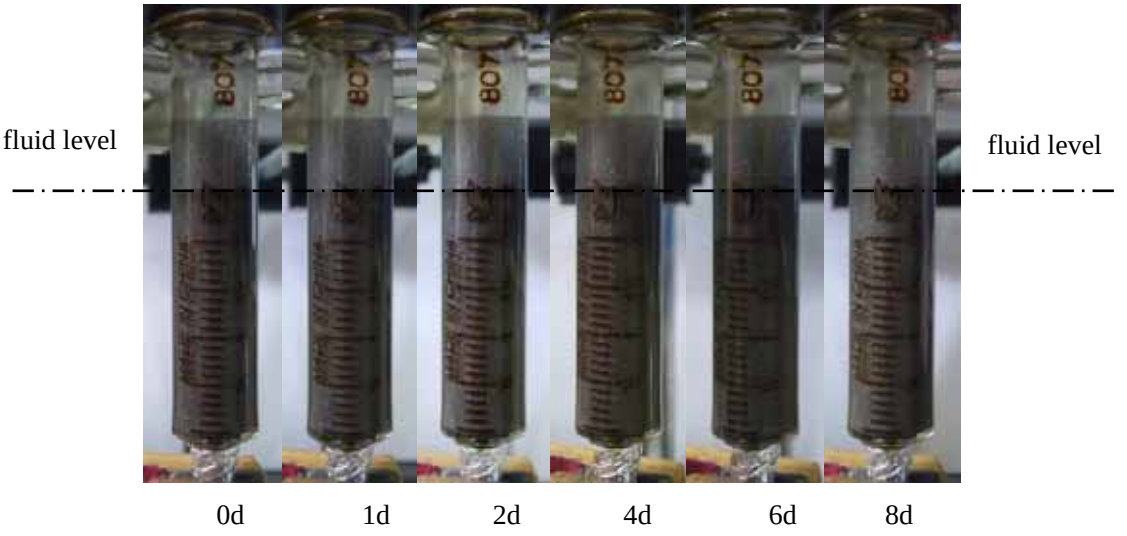

Figure 17: Sedimentation of an MRF, with h_1=24mm and h_2=35mm

particles could not be sufficient to hold it.

The variations of sedimentation ratio against time of the above five tests are shown in Fig. 19. With the decrease of h_1, the sedimentation rate changes remarkably and h_3 (Fig. 12) increases. The sedimentation rate corresponding to h_1=24 mm almost vanishes, indicating that the ferromagnetic particles do not settle distinctly during the whole 8-day testing. Noticing that no additive has been used in the tested MRF sample, this result implies the encouraging application of this method in practice.

Experiment shows clearly that the use of permanent magnets can greatly improve the sedimentation stability of MRFs. Meanwhile, in order to gain the best result in practical application, two requirements need to be satisfied. Firstly, the distribution and the gradient of the magnetic field intensity should match the height and volume of the MRF adopted, thus, different permanent magnets or other proper devices that could provide the required gradient magnetic field should be chosen or developed for different types of MRFs and MRF devices. Secondly, MRF should be placed at a proper position under a permanent magnet, which depends on the properties of both the MRF and the permanent magnet. If the MRF is placed too far from the permanent magnet, the effect would very weak; but if it is too close the permanent magnet, some MRF might be separated from the MRF and adhere to the permanent magnet. Fortunately, this position can be approximately estimated by either numerical simulation or experiment.

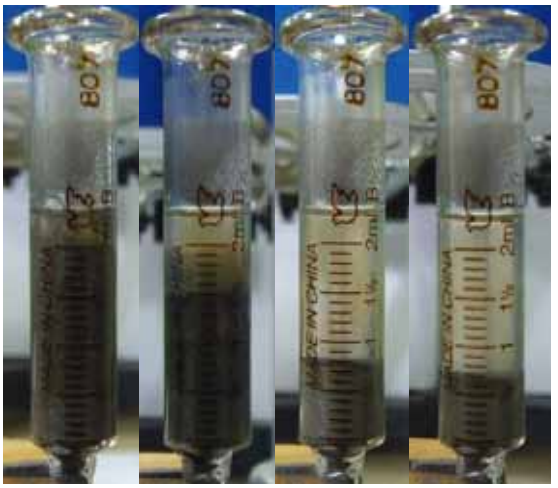

0.04d 0.25d 1d 3d

Figure 18: Sedimentation of MRF sample after the test in Fig. 17, with the permanent magnet removed

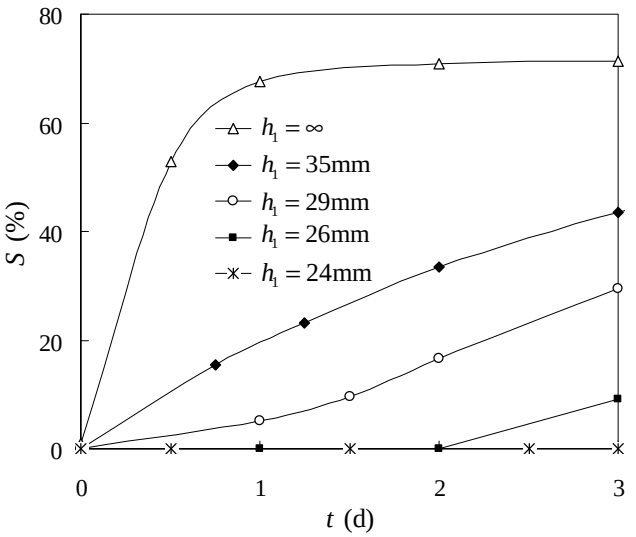

Figure 19: $S-t$ curves of samples

4 Discussions and Conclusions

A new method to improve the sedimentation stability of MRFs by using permanent magnets was investigated with numerical simulation and experiment. The numerical simulation was performed with FE code ANSYS. It was found that in the gradient magnetic field provided by a permanent magnet, there is a point on the vertical central line below the permanent magnet, where the magnetic force on the ferromagnetic particle at this point is equal to the sedimentation force, implying that the particle at this point may stop settling, and the sedimentation of the particle below this point would also decrease markedly. If a group of particles are magnetized by the magnetic magnet, they will form chain-like structures. The computation showed that the magnetic force on the entire chain could be much larger than the sum of the magnetic force on each individual particle located at the identical position, which could extend greatly the available range of the proposed method. The experimental observation also showed that a proper choice of the distance between the permanent magnet and the surface of the MRF sample may greatly reduce and even cease the sedimentation. It should be noted that sedimentation is the bottleneck of the application of MRFs. Since the conventional method of using additives can not solve the problem thoroughly, the proposed method may provide an available solution for this kind of problem.

We like to discuss some worries related to the applicability of the proposed method. For example, since the additional magnet would contribute to the magnetization state of the dispersed particles, should it prevent the suspension from behaving as a liquid-like when needed? Such kind of worry does not seem necessary because of the following two reasons: (1) In an MRF device, the main part of MRF is contained in the chamber(s) where the permanent magnet(s) should be used to avoid sedimentation. And the magnetic field to transform the MRF from a liquid state to a solid-like state is usually applied in a narrow channel, where the sedimentation and its effect are less significant. Therefore, the two magnetic fields can be separated and the interaction between them can be reduced as much as possible by an appropriate design. (2) The magnet field to avoid sedimentation should be much weaker than that to transform an MRF from a viscous state to a solid-like state [Xiong *et al.* (2011)]. On the other word, it can not distinctly change the property of the liquid-like state of an MRF as it is applied individually.

It should also be noted that, in this work, the magnetic force on particles and particle chains is assumed to be generated by a permanent magnet, which is just for the purpose to illustrate the principle and the possibility of the method in reducing sedimentation of MRFs. To implement this method in MRF-based devices such as MR dampers, one may ask if the presence of permanent magnet in most of MR-based systems is practical. In real MRF-based systems, the consideration on

the applicability of this method may involve different cases: (1) for the case as an MRF device is immobile and operated occasionally, such as the MRF dampers used in bridges or buildings to avoid the impact of possible earthquake, this method should be easy and effective; (2) for the case as an MRF device is mobile and operated frequently, such as the MRF dampers used in vehicles, the sedimentation of the MRF with good additives may not be a serious problem, and it does not seem necessary to use additional magnets to avoid sedimentation; and (3) for other cases, we can adopt the proposed method by adjusting some parameters, such as the position of the magnet or its magnetic field intensity (suppose an electrical magnet is used) with an active or adaptive control method.

Acknowledgement: The authors gratefully acknowledge the financial support to this work from the Natural Science Foundation of China under Grant No. 10872220, Chongqing Science and Technology Commission under Grant No. 2011BA4028, and Key Program of the Fundamental Research Funds for the Central Universities under Grant No. CDJXS10242206.

References

Alves S.; Alcantara M. R.; Figueiredo Neto A. M. (2009): The effect of hydrophobic and hydrophilic fumed silica on the rheology of magnetorheological suspensions. *Rheol.*, vol.53, pp. 651-662.

Bossis G. ; Lacis S.; Meunier A.; Volkova O. (2002): Magnetorheological fluids. *Journal of Magnetism and Magnetic Materials*, vol. 252, pp. 224–228.

Carlson J. (2000): Low-cost MR fluid sponge devices. *J. Intell. Mater. Syst. Struct.*, vol.10, pp. 589-594.

Choi H. J.; Park B. J.; Cho M. S.; You J. L. (2007): Core-shell structured poly(methyl methacrylate) coated carbonyl iron particles and their magnetorheological characteristics. *J. Magnetism and Magnetic Materials*, vol. 310, pp. 2835-2837.

Choi J. S.; Park B. J.; Cho M. S.; Choi H. J. (2006): Preparation and magnetorheological characteristics of polymer coated carbonyl iron suspensions. *Journal of Magnetism and Magnetic Materials*, vol. 304, pp. 374–376.

Ekwebelam C.; See H. (2009): Microstructural investigations of the yielding behaviour of bidisperse magnetorheological fluids. *Rheol Acta*, vol. 48, pp. 19–32.

Fang F. F.; Jang I. B.; Choi H. J. (2007): Single-walled carbon nanotube added carbonyl iron suspension and its magnetorheology. *Diamond & Related Materials*, vol. 16, pp. 1167-1169.

Furst E.; Gast A. (2000): Micromechanics of magnetorheological suspensions. *Phys. Rev. E.*, vol.61, pp. 6732-6739.

Janocha H. (2001): Application potential of magnetic field driven new actuators. *Sensors and Actuators*, vol. 91, pp. 126-132.

Jiang W.; Zhang F.; Chen Z.; Gong X. (2006): Carbonyl iron modified with nano cobalt and its magnetorheological effect. *Journal of Functional Materials*, vol. 37, pp. 1163-1165.

Jin G.; Sain M.; Spencer B. (2005): Nonlinear black box modeling of MR-dampers for civil structural control. *IEEE Transactions on Control Systems Technology*, vol. 13, pp. 345-355.

Keaveny E.; Maxey M. (2008): Modeling the magnetic interactions between paramagnetic beads in magnetorheological fluids. *Journal of Computational Physics*, vol. 277, pp. 9554-9571.

Li H.; Peng X.; Chen W. (2005): Simulation of the Chain-formation Process in Magnetic Fields. *J. Intelligent Material Systems and Structures*, vol. 16, pp. 653-658.

Li H.; Peng X.; Huang S. (2008): Study on the chain formation mechanism of magnetorheological fluids based on dipole theory. *Journal of Functional Materials*, vol. 6, pp. 902-904.

López-López M. T.; de Vicente J.; González-Caballero F.; Durán J. D. G. (2007): Stability of magnetizable colloidal suspensions by addition of oleic acid and silica nanoparticles. *Colloids and Surfaces A: Physicochemical and Engineering Aspects*, vol. 264, pp. 75–81.

López-López M. T.; Kuzhir P.; Bossis G.; Bossis G.; Mingalyov P. (2008): Preparation of well-dispersed magnetorheological fluids and effect of dispersion on their magnetorheological properties. *Rheol. Acta*, vol. 47, pp. 787–796.

López-López M. T.; Zugaldía A.; González-Caballero F.; Durán J. D. G. (2006): Sedimentation and redispersion phenomena in iron-based magnetorheological fluids. *J. Rheol.*, vol.50, pp. 543-560.

Luo X.; Liu S. (2007): Preparation and chemical stability of iron-nitride-coated iron microparticles. *Journal of Magnetism and Magnetic Materials*, vol. 308, pp. L1–L4.

Ly H. V.; Reitich F.; Jolly M. R.; Banks H. T.; Ito K. (1999): Simulations of particle dynamics in magnetorheological fluids. *Journal of Computational Physics*, vol. 155, pp. 160-177.

Murashov Vladimir V.; Pateya G. N. (2006): Structure formation in dipolar fluids driven by rotating fields. *Journal of Chemical Physics*, vol. 112, pp. 9828-9833.

Park B. J.; Jang I. B.; Choi H. J.; Pich A.; Bhattacharya S.; Adler H-J. (2006): Magnetorheological characteristics of nanoparticle-added carbonyl iron system. *Journal of Magnetism and Magnetic Materials*, vol. 303, pp. 290-293.

Peng X.; Li H. (2007): Analysis of the magnetomechanical behavior of MRFs based on micromechanics incorporating a statistical approach. *Smart Mater. Struct*., vol. 16, pp. 2477-2485.

Pu H.; Feng J.; Yang Z. (2006): Preparation and properties of soft magnetic particles based on Fe_3O_4 and hollow polystyrene microsphere composite. *Materials Chemistry and Physics*, vol. 100, pp. 10-14.

Rong Y.; Tao R.; Tang X. (2000): Flexible fixturing with phasechange materials Part 1 experimental study on magnetorheological fluids. *International Journal of Advanced Manufacturing Technology*, vol. 16, pp. 822-829.

Tang X.; Zhang X.; Tao R. (2000): Structure-enhanced yield strength of MR fluids. *Journal of Applied Physics,* vol. 87, pp. 2634-2638.

Viota J. L.; González-Caballero F.; Durán J.; Delgado A. V. (2007): Study of the colloidal stability of concentrated bimodal magnetic fluids. *Journal of Colloid and Interface Science*, vol, 309, pp. 135-139.

Xiong C.; Peng X.; Yi C. (2011): Experimental investigation to effects of oleic acid and lauric acid on stabilization of magnetorheological fluids. *Journal of Functional Materials*, vol. 8, pp. 1504-1507.

Yang Y.; Li L.; Chen G.; Li W. (2006): Magnetorheological properties of aqueous ferrofluids. *Journal of the Japanese Society of Rheology*, vol. 34, pp.25-31.

Zhu Y.; Haddadian E.; Mou T.; Gross M.; Liu J. (1996): Role of nucleation in the structure evolution of a magnetorheological fluid. *Phys. Rev. E*., vol. 53, pp. 1753-1759.